Video Article

MRI and PET in Mouse Models of Myocardial Infarction

Guido Buonincontri[1], Carmen Methner[2], T. Adrian Carpenter[1], Robert C. Hawkes[1], Stephen J. Sawiak[1,3], Thomas Krieg[2]

[1]Wolfson Brain Imaging Centre, Department of Clinical Neurosciences, Unversity of Cambridge

[2]Department of Medicine, University of Cambridge

[3]Behavioural and Clinical Neurosciences Institute, University of Cambridge

Correspondence to: Thomas Krieg at

URL: http://www.jove.com/video/50806
DOI: doi:10.3791/50806

Keywords: Medicine, Issue 82, anatomy, Late Gadolinium Enhancement (LGE), MRI, FDG PET, MRI/PET imaging, myocardial infarction, mouse model, contrast agents, coregistration

Date Published: 12/19/2013

Citation: Buonincontri, G., Methner, C., Carpenter, T.A., Hawkes, R.C., Sawiak, S.J., Krieg, T. MRI and PET in Mouse Models of Myocardial Infarction. *J. Vis. Exp.* (82), e50806, doi:10.3791/50806 (2013).

Abstract

Myocardial infarction is one of the leading causes of death in the Western world. The similarity of the mouse heart to the human heart has made it an ideal model for testing novel therapeutic strategies.

In vivo magnetic resonance imaging (MRI) gives excellent views of the heart noninvasively with clear anatomical detail, which can be used for accurate functional assessment. Contrast agents can provide basic measures of tissue viability but these are nonspecific. Positron emission tomography (PET) is a complementary technique that is highly specific for molecular imaging, but lacks the anatomical detail of MRI. Used together, these techniques offer a sensitive, specific and quantitative tool for the assessment of the heart in disease and recovery following treatment.

In this paper we explain how these methods are carried out in mouse models of acute myocardial infarction. The procedures described here were designed for the assessment of putative protective drug treatments. We used MRI to measure systolic function and infarct size with late gadolinium enhancement, and PET with fluorodeoxyglucose (FDG) to assess metabolic function in the infarcted region. The paper focuses on practical aspects such as slice planning, accurate gating, drug delivery, segmentation of images, and multimodal coregistration. The methods presented here achieve good repeatability and accuracy maintaining a high throughput.

Video Link

The video component of this article can be found at http://www.jove.com/video/50806/

Introduction

In order to measure the efficacy of new treatment strategies for myocardial infarction (MI) in preclinical studies, the assessment of the acute stage as well as long-term outcome is required[1]. Methods such as histopathology, intracardiac catheters[2], and *ex vivo* heart models[3] are commonly used for preclinical studies in mice. It is impossible, however, to follow up treatment with *ex vivo* or highly invasive methods. Noninvasive measurement techniques as *in vivo* magnetic resonance imaging (MRI) and positron emission tomography (PET) allow longitudinal experimental designs for disease staging in single subjects. Cine-MRI is used to derive global functional parameters such as left ventricular mass (LVM), ejection fraction (EF) and cardiac output (CO). In addition, after the injection of a gadolinium contrast agent, due to impaired perfusion and washout in the infarction, tissue viability can be assessed with late gadolinium enhancement (LGE) MRI. Complementarily, PET offers a sensitive measure of radiolabeled molecules in order to assess tissue metabolism. The high accuracy of these techniques permits significant reductions in the number of animals required for testing new drugs targeting MI.

The PET and MRI procedures are involved, and without a carefully designed protocol reproducibility is hard to maintain. Procedures established in the clinic for patients require substantial modification for use in mice, due to their considerably faster heart rate and smaller dimensions of the heart[4]. There is wide variation between individual subjects, both at baseline and in response to induced injury, so a considerable number of mice are needed to establish treatment efficacy.

In this report, we describe our method for sequential PET/MRI imaging of the mouse heart. Both modalities use intravenous contrast agents, which are delivered through the tail vein. MRI consists of standard assessment with Cine-MRI[5] with an optimal protocol for LGE as described in our previous work[6]. The entire MRI procedure lasts 30 min. We have obtained consistent fittings for the beds of our instruments so it is possible to transfer the animal on a platform with the same monitoring and anesthetic delivery apparatus between the machines. The PET scan lasts 45 min with *in situ* injection once the scan is started. The final step is to measure the parameters from both MRI and PET images following coregistration.

Protocol

All components of this study were carried out in accordance with the UK Animals (Scientific Procedures) Act, 1986, and with the approval of the University of Cambridge Ethical Review Panel.

1. Animal Preparation

1. Induce infarcts with a surgical intervention[7,8]. For measuring at the acute stage, perform imaging 24 hr after intervention.
2. Prepare a thin syringe tubing for drug delivery with a 25 G needle at one extremity and a syringe with a 25 G needle at the other end. The length of the line should be enough to allow the injection from outside the magnet's bore (approximately 1.5 m).
3. Prepare a solution diluting Gadovist in saline. Load a syringe with the right amount of solution to achieve 3 mmol/kg adjusted for mouse bodyweight. Keep the injection volume between 50-100 µl.
4. Prefill the line with the Gadovist solution. To avoid blood clotting, fill the extremity of the line close to the cannula with heparin saline.
5. Place the mouse in the induction box for anesthesia with 3% isoflurane in O_2 1 L/min for 3-5 min as necessary. Correct anesthesia depth can be identified with the slowing breath rate, which should decrease to less than 70 bpm.
6. Cannulate the tail vein using the line previously prepared, use surgical tape to keep the needle in place during the procedure.

2. Animal Positioning and Monitoring

1. Place the mouse on the MRI bed, delivering 1-2% isoflurane in 1 L/min O_2 for anesthesia maintenance as required. Maintain respiration rates between 20-70 bpm.
2. Ensure the center of the MRI coil is located over the mouse heart position.
3. Monitor respiration by placing a respiratory pillow sensor slightly below the diaphragm. Use a rectal thermometer with a prelubricated cover slip to monitor core temperature. Ensure that temperature is kept constant during the scans at 37±2 °C.
4. For ECG monitoring, place three electrodes on the anterior paws and on the left rear paw, making sure that the palm of the toe is completely open. Choose the pair of electrodes achieving the best signal quality to derive the ECG. Twist the ECG cables together, to insure that they do not form resonant circuits at the MRI resonant frequency, which would severely corrupt the ECG signal when running pulse sequences.
5. Ensure the electrodes are firmly attached to the bed using tape. The electrodes and the nose cone will hold the animal in place during the whole procedure.
6. Position a water-heated blanket over the mouse, encapsulating the monitoring and coil leads to maintain body temperature.
7. Align the laser of the bed with the heart position; use the anterior toes line as a landmark. Position this in the magnet isocenter using an automatic bed.
8. Run the standard adjustments for the MRI system.
9. Set the monitoring equipment to detect the R-wave in the ECG. Adjust the thresholds for each mouse and within imaging sessions so that there is reliable triggering.

3. MRI

1. Acquire a pilot image to plan the multiplanar pilot images.
2. Identify the heart in the image, most easily by its flow artifacts. If the images show the mouse is not well centered in the coil or the isocenter, retract the bed and repeat positioning.
3. Acquire a fast gradient echo (GE) image with five slices per orientation and a 3 cm field of view (FOV) with ECG gating turned on.
4. Run an ungated 3D scan centered on the heart for PET coregistration (see **Table 1** for scan parameters). While this scan is running, plan the successive scans.
5. Plan a four chamber (4 ch) view scan (see **Table 1** for scan parameters). This should cut through the apex and the tricuspid and mitral valves, showing all 4 chambers.
6. Plan a two chamber (2 ch) view (see **Table 1** for scan parameters). It should cut through the apex and the tricuspid valve, showing the left atrium and ventricle.
7. Crosscheck the geometry of the two long-axis views. If the slice planning is sub-optimal, repeat the scan.
8. Plan a stack of short axis slices (see **Table 1** for scan parameters) orthogonal to both the 4 ch and to the 2 ch view. Cover the whole heart, starting from the first apical slice without blood pool until the first basal slice without any RV. Slices should be equally spaced with no gaps.

4. Late Gadolinium Enhancement

1. Increase blank time for gating to acquire every other heart beat (TR = 550-750 msec). A delay must be applied such that acquisition is performed at the end-diastolic phase of the ECG.
2. Perform a low-resolution version of the LGE sequence (see **Table 1** for scan parameters) before the injection in order to check that the gating is correct and no flow artifacts are present. If flow artifacts are present in the diastolic phase, increasing the delay slightly (*i.e.* imaging at the very early stage of systole) will get rid of them.
3. Perform the injection of the Gadovist solution slowly and steadily over 15 sec.
4. Initiate LGE imaging (see **Table 1** for scan parameters) after the injection. Good contrast is achieved when imaging within the first 15 min.

5. PET Imaging

1. Transfer the MRI bed to the PET scanner leaving the receiver in place and firmly anchor it to the PET bed support. Connect the anesthetic and monitoring equipment.
2. Position the heart in the center of the PET field of view moving the bed only axially.
3. Acquire a single-pass transmission scan with a germanium source.
4. Extract 10-30 Mbq of radioactively labeled FDG from its container with a syringe. Take necessary care with radioactive material. Measure the activity with a well counter. A good injection volume for mice ranges between 50-100 µl, if the volume is too small, dilute the solution with saline.
5. Start the emission scan, set to acquire list-mode gated PET for 45 min. Contemporaneously, inject the tracer slowly and steadily over 15 sec. Flush the line with enough saline to deliver the whole of the radioactive tracer.
6. For animal health, do not to exceed 300 µl with the three injections (*i.e.* Gadovist, FDG, flush).
7. Place the syringe back in the well counter to measure the residual activity.
8. Follow local rules throughout for handling radioactive material.

6. MRI Segmentation

1. Load the Cine-MRI images in Segment v1.9 [9].
2. Run the automatic tools for segmentation. Starting from a point inside the ventricle, these will inflate the estimated ventricle walls until the best match is found.
3. Delineate the LV and the RV manually at end systole (ES) and end diastole (ED), defined respectively as the frames with the maximal and with the minimal global LV volume. Exclude the papillary muscles and trabeculations throughout. Do not adjust image contrast, as inconsistency in the contrast leads to a different interpretation of partial volume effects.
4. Delineate manually the epicardium at ES and ED for LV mass calculations, as shown in **Figure 6**. The cardiac muscle is incompressible, so the LV mass must be consistent in ES and ED. If the difference is more than 5% operator error is likely and these should be reviewed.
5. At the base of the ventricles, use a straight line to discriminate ventricles from atria as shown in **Figure 6**, identifying the angle of the slice with the help of the long-axis views.
6. Cross-check the segmentation on the long-axis views.
7. Delineate the scar area on the LGE images. Divide the scar volume by the LV mass derived in the cine imaging to obtain the infarct as a percentage of the LV.

7. PET Analysis and Coregistration with MRI

1. Reconstruct the PET images using a 3D filtered backprojection algorithm and export data to Nifti format (http://nifti.nimh.nih.gov/) showing standard uptake values.
2. Transform all the PET images using the fixed transformation matrix between the PET and the MRI system. If the matrix is not known, fill a geometrical phantom with radioactive material and perform an MRI, then move the bed to the PET and perform an emission scan. The matrix obtained to transform the PET to the MRI image is the standard matrix to go from the PET to the MRI system.
3. Register the average PET image to the 3D MRI using SPM-mouse bulk coregistration tool[10].
4. Stack the slices from Cine-MRI to obtain a 3D reconstruction, interpolate to obtain 0.3 mm isotropic resolution. Register the end-diastolic PET volume to the end-diastolic MRI volume using SPM-Mouse coregistration tools. Use the same matrix for all the other heart phases.
5. To evaluate PET infarct size, choose 50% of the maximum intensity in the heart to discriminate between infarcted and noninfarcted voxels. Express infarcted voxels as a percentage of the LV.

Representative Results

One of the advantages of using MRI is that a longitudinal design can be used in order to stage disease. This is especially important when evaluating novel compounds, as the time course of effect may not be known. Variations in heart volumes due to the disease progression in the same animal are shown in **Figure 4**. The figure clearly shows the effects of remodeling post myocardial infarction.

Correct slice geometry is crucial for the success of a cardiac MRI experiment. Representative slice planning and resulting geometry for various MRI scans are reported in **Figure 5**. Segmentation of two MRI short-axis slices is shown in **Figure 6**. Our Cine-MRI procedure achieved a precision of 4% for LV mass, 3% for EDV, 5% for ESV, 2% for SV, 2% for EF, and 4% for infarct size (coefficient of variation, measured on $n = 4$ wild-type mice with both, data acquisition and segmentation procedure, repeated 2x for each animal).

PET can be used to measure the binding of specific tracers throughout the body. An example of FDG-PET maximum intensity projection image is shown in **Figure 7**. As expected, in an anesthetized animal, the greatest uptake is found in the heart and in the brain. **Figure 8** shows coregistered LGE MRI and FDG-PET. The enhanced areas on MRI, representing nonviable tissue, match areas of reduced FDG uptake in the PET.

Scan	Sequence
Cine imaging	FISP, TR/TE 7 msec/2.4 msec, frames 13-20, matrix 256 x 256 x 128 with FOV 3.5 cm, slice thickness 1 mm, bandwidth 64 kHz, flip angle 20°, NEX 2
3D scan for coregistration	FISP, FISP, TR/TE 8 msec/4 msec, matrix 256 x 256 x 128, FOV 3 x 3 x 6.40 cm, bandwidth 50 kHz, flip angle 15°, NEX 2
Scout before injection	FLASH, FOV 3.5 cm, matrix 128 x 128, slice thickness 0.8 mm with 0.2 mm gap between adjacent slices TE = 2.8 msec, TR = 550-750 msec, FLASH TR 7 msec, bandwidth 64 kHz, flip angle 60°, 1 NEX, 0.8 mm, 0.2 mm gap, selective inversion 0.8 mm thickness with 5 msec sech shaped pulse
LGE imaging	FLASH, FOV 3.5 cm, matrix 256 x 256, slice thickness 0.8 mm with 0.2 mm gap between adjacent slices TE = 2.8 msec, TR = 550-750 msec, FLASH TR 7 msec, bandwidth 64 kHz, flip angle 60°, 1 NEX, 0.8 mm, 0.2 mm gap, selective inversion 0.8 mm thickness with 5 msec sech shaped pulse

Table 1. MRI sequences. Abbreviations are FISP: fast imaging with steady state precession; FLASH: fast low angle shot; TE: echo time; TR: repetition time; NEX: number of excitations.

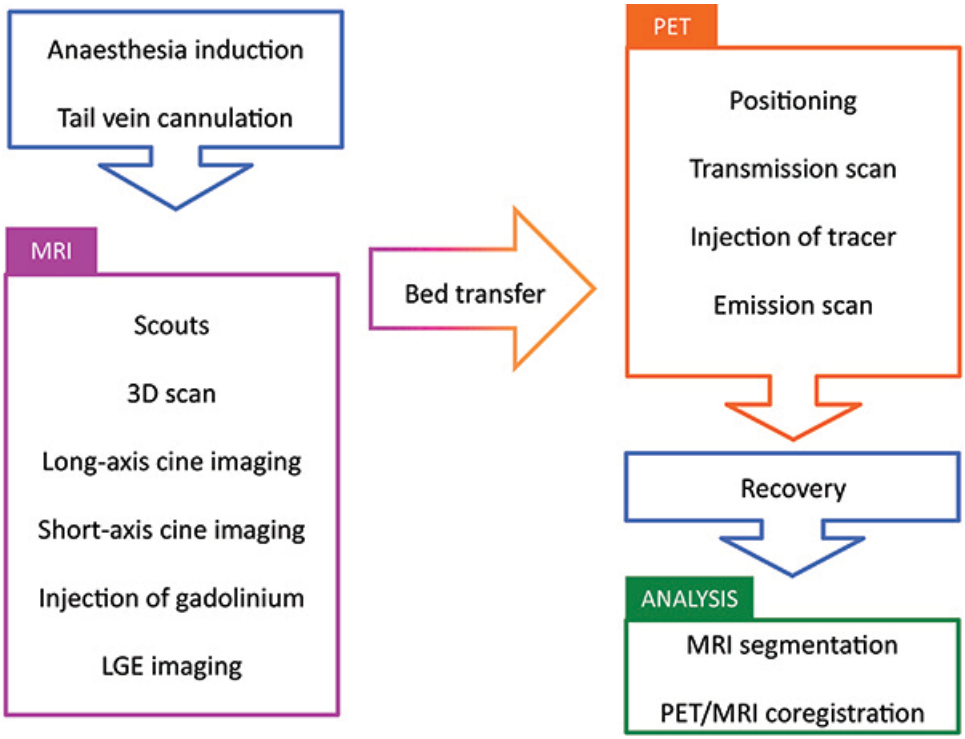

Figure 1. Overview of the experiment. Click here to view larger image.

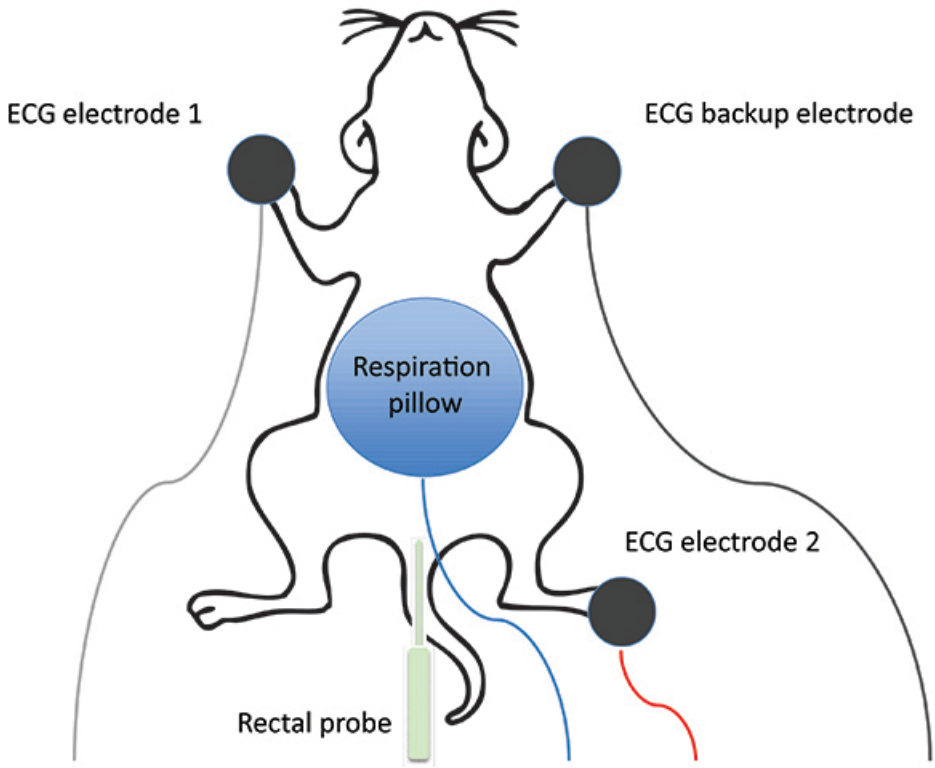

Figure 2. Animal monitoring setup. ECG is derived with graphite electrodes on the paws, respiration with a pillow under the chest connected to a piezoelectric transducer and temperature with a lubricated rectal probe. Click here to view larger image.

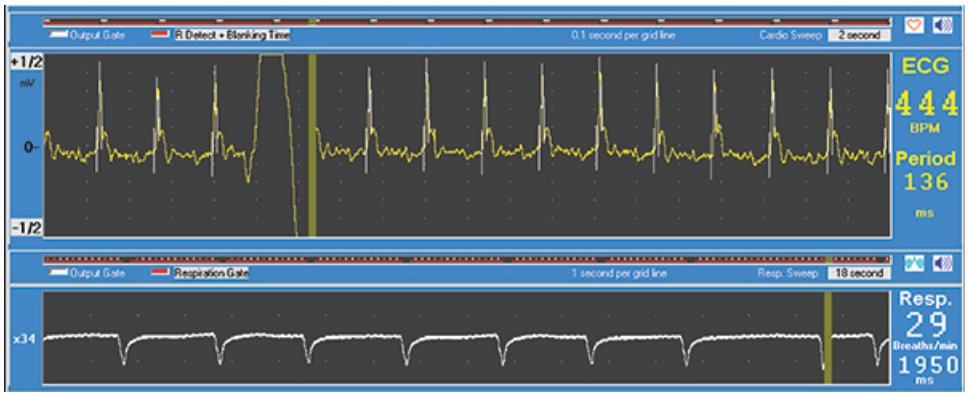

Figure 3. Representative monitoring and gating traces. Anesthetic dose should be adjusted to achieve stable traces during the exams. Click here to view larger image.

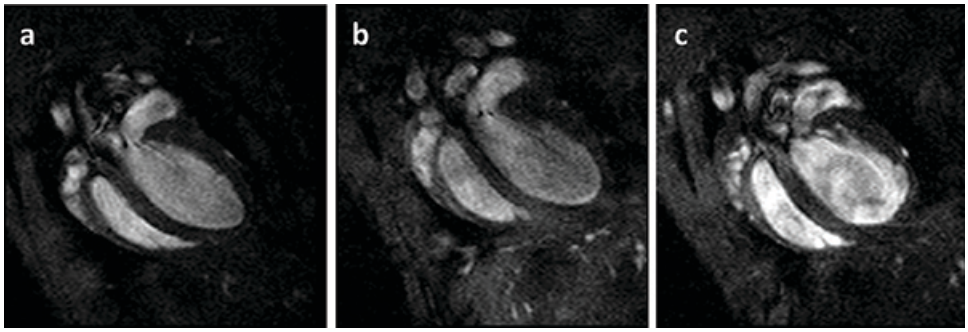

Figure 4. a) **End-diastolic 4 ch view of a mouse at baseline. b**) End-diastolic 4 ch view of the same mouse one day after induced injury. **c**) End-diastolic 4 ch view of the same mouse four weeks after induced injury. Click here to view larger image.

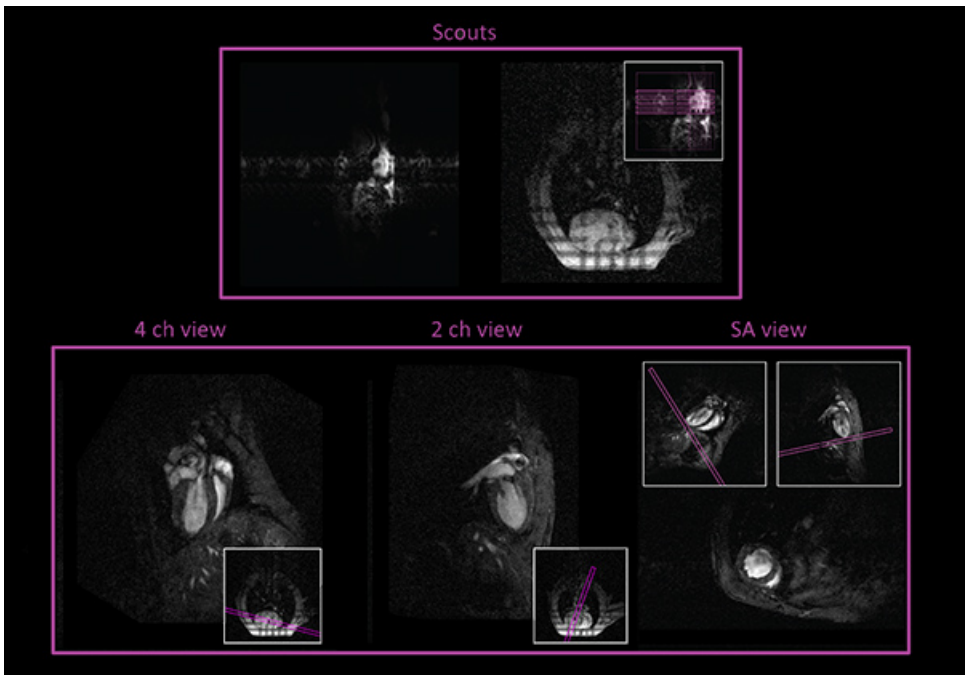

Figure 5. Slice planning and resulting images for the relevant views in cine MRI. A correct slice geometry is key in achieving reproducible measurements. Click here to view larger image.

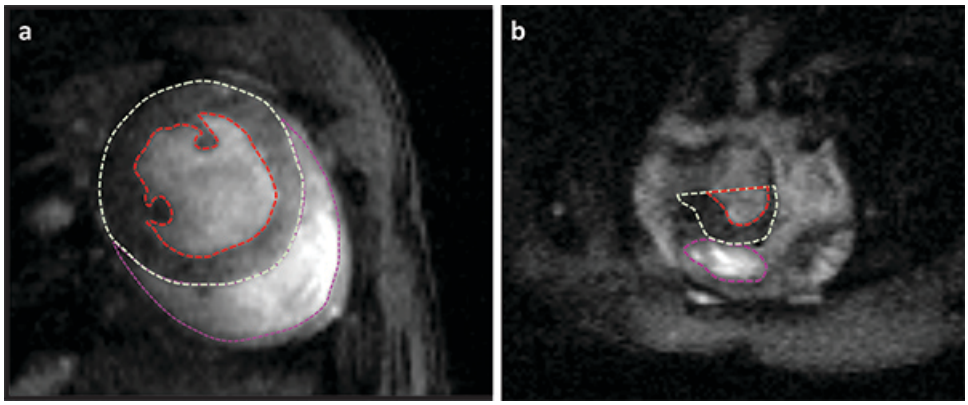

Figure 6. a) **Segmentation of a mid-ventricular short-axis slice. b**) Segmentation of a basal short-axis slice. Endocardial and epicardial borders are identified and segmented for each short-axis slice. Fixed rules must be applied to achieve reproducible volume estimates. Click here to view larger image.

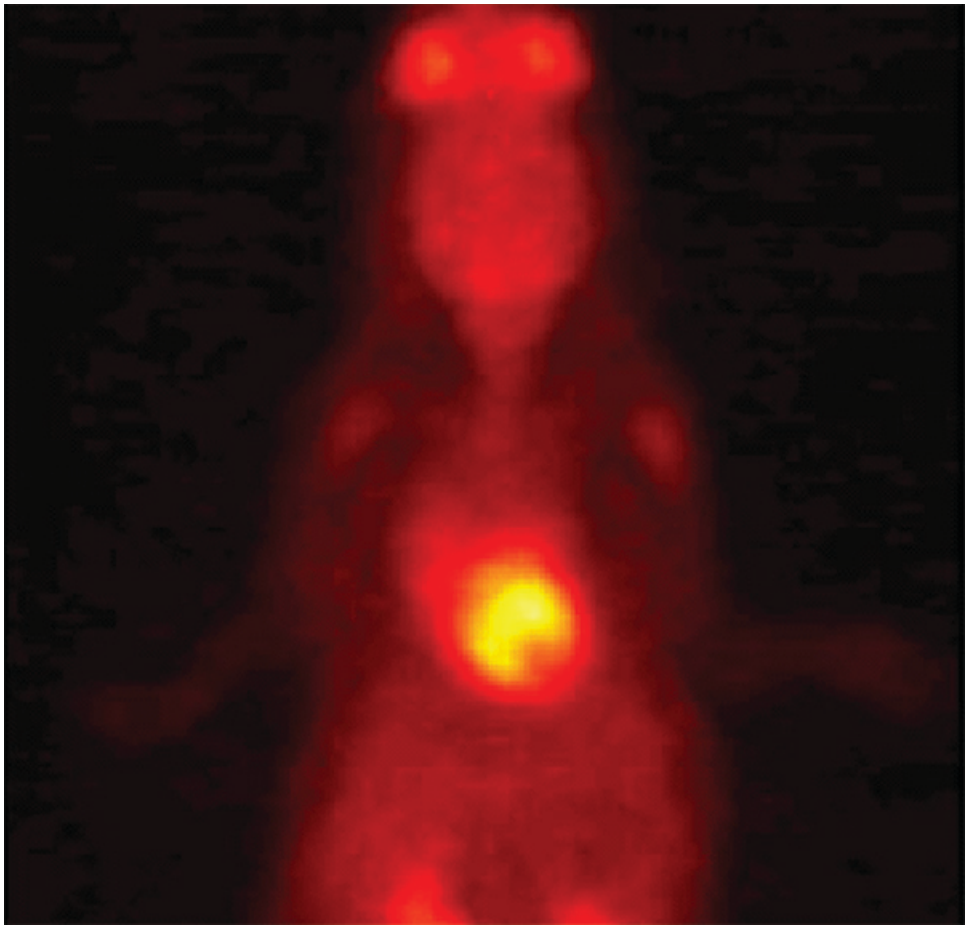

Figure 7. Maximum intensity projection of an FDG-PET scan. Higher uptake is seen in areas that are more metabolically active. Click here to view larger image.

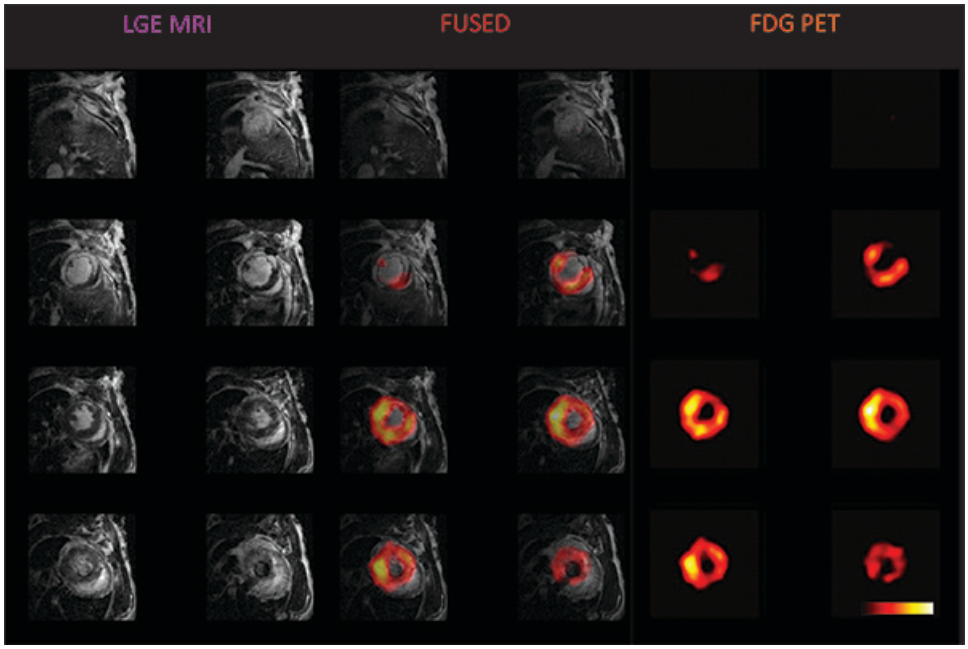

Figure 8. Coregistration between LGE MRI and FDG PET. There is good agreement between the two techniques in identifying viable tissue. Click here to view larger image.

Discussion

PET/MRI is a comprehensive measurement method for the noninvasive and longitudinal evaluation of systolic function, tissue viability and specific metabolic markers in mouse models of myocardial infarction. Here we have described a protocol for performing MRI and PET sequentially, where coregistration is simplified by the transfer of the same bed between systems. This strategy, also adopted by manufacturers of clinical systems[11], does not require a combined PET/MRI scanner and can be performed with standard equipment. After measuring the fixed matrix for transformation between the two systems, coregistration of the PET with the MRI data is obtained with an axial translation. This simplification is particularly useful in cardiac studies, where coregistration is complicated by motion.

This protocol can be performed using a number of different commercially available scanners. Different PET cameras can be used, as long as a proper connection of the MRI bed to the PET allows accurate positioning. If the pulse sequences are properly modified, it is also possible to perform the MRI measurements at different field strengths[12-15,] on small bore as well as clinical systems[16]. Although at 4.7 TECG signal quality could be insured by placing the electrodes with care, this might not always work at higher field strengths where self-gating technologies might be needed[17].

To obtain a good outcome, particular attention should be paid to some critical steps of the protocol. First, slice planning and gating for MRI of the mouse heart, as sub-optimal geometry or gating produce inconsistent data that cannot be corrected in post-processing. Secondly, segmentation of MRI data, which is performed in post-processing and can be repeated multiple times, but rigorous and fixed rules must be applied in order to avoid biases in the volume estimates. Thirdly, transfer between different scanners, where motion should be avoided, to exclude a mismatch between the final images. Last, keep the injection volumes low, especially as three injections are performed during the whole procedure. To avoid sub optimal injections, specific activity of the PET tracer should be measured before initiating imaging, to ensure that enough activity can be injected maintaining low volumes.

The main limitation of our procedure is that PET and MRI are not performed simultaneously but sequentially. This feature does not guarantee complete coregistration of the myocardial wall between modalities, as intravenous injections and time under anesthesia might perturb heart function. However, this effect was not directly observable in our images, which showed excellent match between techniques. A comparison with novel simultaneous PET/MRI technologies would be needed to quantify this effect and to assess its relevance. Although some preliminary results have been reported with isochronous PET/MRI in the mouse heart[18,19], customized scanners to perform this exam are still not widely available, and most groups are forced to perform MRI and PET sequentially. With simultaneous PET/MRI still in its infancy, reliable sequential methods such as the one described in this paper are needed to perform multimodal imaging.

Imaging techniques represent a valuable tool for assessment of new therapies *in vivo,* which can substitute more invasive techniques. MRI and PET can be used to assess left ventricular morphology, tissue viability and metabolism in mouse models of heart disease[20]. MRI provides an alternative to terminal procedures to assess LV function, such as intracardiac pressure-volume loop measurements[2] or the *ex vivo* working heart model[3]. Assessment of LV chamber dimensions with MRI allows for detection of abnormal LV chamber enlargement or increased wall thickness[4]. Tissue viability can be noninvasively measured with LGE, achieving results in good agreement with TTC staining[6]. FDG-PET one day after infarction provides glucose metabolism at the aftermath of the ischemic insult, showing areas that are still metabolically functional[20]. Using imaging methods can significantly contribute to refinement and reduction in animal research.

Future applications of this imaging method include basic science studies on biochemical processes in the injured heart, assessment of novel pharmaceutical agents, and evaluation of new PET tracers. Noninvasive methods of targeting biochemical properties of tissue can be performed longitudinally to monitor remodeling, inflammation[21] and drug efficacy in the long term.

Disclosures

There is nothing to disclose.

Acknowledgements

We are grateful for funding from the British Heart Foundation to TK and to the UK Medical Research Council for a postgraduate research studentship to GB.

References

1. Borst, O. *et al.* Methods employed for induction and analysis of experimental myocardial infarction in mice. *Cell. Physiol. Biochem.* **28**, 1-12, doi:10.1159/000331708 (2011).
2. Pacher, P., Nagayama, T., Mukhopadhyay, P., Bátkai, S. & Kass, D. A. Measurement of cardiac function using pressure-volume conductance catheter technique in mice and rats. *Nat. Protoc.* **3**, 1422-1434, doi:10.1038/nprot.2008.138 (2008).
3. Larsen, T. S. *et al.* The isolated working mouse heart: methodological considerations. *Pflügers Arch.* **437**, 979-985 (1999).
4. Epstein, F. H. MR in mouse models of cardiac disease. *NMR Biomed.* **20**, 238-255, doi:10.1002/nbm.1152 (2007).
5. Schneider, J. E., Wiesmann, F., Lygate, C. A. & Neubauer, S. How to perform an accurate assessment of cardiac function in mice using high-resolution magnetic resonance imaging. *J. Cardiov. Magn. Reson.* **8**, 693-701, doi:10.1080/10976640600723664 (2006).
6. Buonincontri, G., Methner, C., Krieg, T., Carpenter, T. A. & Sawiak, S. J. A fast protocol for infarct quantification in mice. *J. Magn. Reson. Imaging.* doi:10.1002/jmri.24001 (2013).
7. Methner, C., Schmidt, K., Cohen, M. V., Downey, J. M. & Krieg, T. Both A2a and A2b adenosine receptors at reperfusion are necessary to reduce infarct size in mouse hearts. *Am. J. Physiol.* **299**, H1262-1264, doi:10.1152/ajpheart.00181.2010 (2010).

8. Methner, C. *et al.* Protection through postconditioning or a mitochondria-targeted S-nitrosothiol is unaffected by cardiomyocyte-selective ablation of protein kinase G. *Basic. Res. Cardiol.* (in press) (2013).
9. Heiberg, E. *et al.* Design and validation of Segment--freely available software for cardiovascular image analysis. *BMC Med. Imaging.* **10**, 1, doi:10.1186/1471-2342-10-1 (2010).
10. Sawiak, S. J., Wood, N. I., Williams, G. B., Morton, A. J. & Carpenter, T. A. Voxel-based morphometry in the R6/2 transgenic mouse reveals differences between genotypes not seen with manual 2D morphometry. *Neurobiol. Dis.* **33**, 20-27, doi:10.1016/j.nbd.2008.09.016 (2009).
11. Zaidi, H. *et al.* Design and performance evaluation of a whole-body Ingenuity TF PET-MRI system. *Phys. Med. Biol.* **56**, 3091-3106, doi:10.1088/0031-9155/56/10/013 (2011).
12. Thomas, D. *et al.* T1-weighted cine FLASH is superior to IR imaging of post-infarction myocardial viability at 4.7T. *J. Cardiov. Magn. Reson.* **8**, 345-352 (2006).
13. Protti, A., Sirker, A., Shah, A. M. & Botnar, R. Late gadolinium enhancement of acute myocardial infarction in mice at 7T: cine-FLASH versus inversion recovery. *J. Magn. Reson. Imaging.* **32**, 878-886, doi:10.1002/jmri.22325 (2010).
14. Bohl, S. *et al.* Advanced methods for quantification of infarct size in mice using three-dimensional high-field late gadolinium enhancement MRI. *Am. J. Physiol.* **296**, H1200-1208, doi:10.1152/ajpheart.01294.2008 (2009).
15. Chapon, C., Herlihy, A. H. & Bhakoo, K. K. Assessment of myocardial infarction in mice by late gadolinium enhancement MR imaging using an inversion recovery pulse sequence at 9.4T. *J. Cardiov. Magn. Reson.* **10**, 6, doi:10.1186/1532-429X-10-6 (2008).
16. Price, A. N. *et al.* Cardiovascular magnetic resonance imaging in experimental models. *The open cardiov medicine journal.* **4**, 278-292, doi:10.2174/1874192401004010278 (2010).
17. Hiba, B., Richard, N., Thibault, H. & Janier, M. Cardiac and respiratory self-gated cine MRI in the mouse: comparison between radial and rectilinear techniques at 7T. *Magn. Reson. Med.* **58**, 745-753, doi:10.1002/mrm.21355 (2007).
18. Buonincontri, G. *et al.* PET/MRI in the infarcted mouse heart with the Cambridge split magnet. *Nucl. Instrum. Methods Phys. Res. A.* doi:10.1016/j.nima.2012.07.061 (2012).
19. Büscher, K. *et al.* Isochronous assessment of cardiac metabolism and function in mice using hybrid PET/MRI. *J. Nucl. Med.* **51**, 1277-1284, doi:10.2967/jnumed.110.076448 (2010).
20. Berr, S. S. *et al.* Images in cardiovascular medicine. Serial multimodality assessment of myocardial infarction in mice using magnetic resonance imaging and micro-positron emission tomography provides complementary information on the progression of scar formation. *Circulation.* **115**, e428-429, doi:10.1161/CIRCULATIONAHA.106.673749 (2007).
21. Lee, W. W. *et al.* PET/MRI of inflammation in myocardial infarction. *J. Am. Coll. Cardiol.* **59**, 153-163, doi:10.1016/j.jacc.2011.08.066 (2012).
22. Lucas, A. J. *et al.* Development of a combined microPET-MR system. *Technol. Cancer Res. Treat.* **5**, 337-341 (2006).
23. Hawkes, R. C., Fryer, T. D., Siegel, S., Ansorge, R. E. & Carpenter, T. A. Preliminary evaluation of a combined microPET-MR system. *Technol. Cancer Res. Treat.* **9**, 53-60 (2010).

